Hydrogen bubble visualization of viscoelastic flow in a model of the carotid artery bifurcation

Hydrogen bubble visualization of viscoelastic flow in a model of the carotid artery bifurcation

T.F. van Kampen
February 1996
WFW 96-110

coaches: Dr. Ir. F.N. van de Vosse
Ir. F. Gijsen

Laboratory of Biomechanics
Department of Mechanical Engineering
Eindhoven University of Technology

CONTENTS

1. INTRODUCTION 2

2. MATERIALS AND METHODS 4

2.1. Model of the bifurcation 4

2.2. Visualization of the flow 4

2.3. Blood Analog fluid 5

2.4. Experimental set up 7

2.5. Experimental procedures 8

3. RESULTS 10

4. DISCUSSION AND CONCLUSION 12

5. REFERENCES 14

1. Introduction

Atherosclerosis is a complex arterial disease that is one of the most important causes of death in western countries. The disease is characterized by intimal thickening of the arteries. The thickening of the arterial walls is followed by the plaque formation by small cells such as cholesterol, lipids and other cells. The formation of plaques can lead to partial or complete obstruction of the vessels. Furthermore thrombi can break loose and can get stuck downstream in smaller arteries causing ischemic attacks.
Atherosclerosis can often be found at locations where the flow is disturbed such as bifurcations and bends, e.g. at the carotid artery bifurcation. The carotid artery bifurcation is located in the human neck. The main blood supply to the head, neck and face is through the two (left and right) common carotid arteries, which bifurcate in the external carotid and the internal carotid branches. The external branch supplies blood to the face, neck and top of the head. The brain and the eye are supplied with blood by the internal branch. The internal branch has a widening, called the carotid sinus or bulbus. From clinical practice it is known that atherosclerosis occurs preferentially at the so called non-divider wall in the carotid sinus (see figure 1).

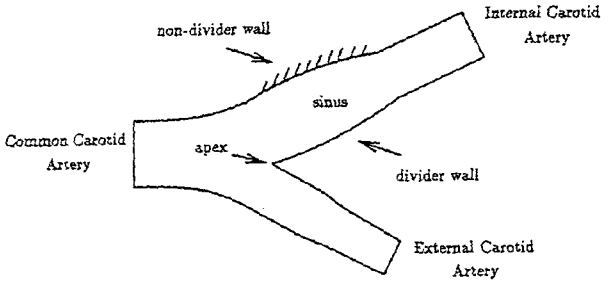

Figure 1, Schematic overview of the carotid artery bifurcation

It is known that there are two processes that mainly cause the development of stenoses: low or oscillating wall shear stresses and diffusion processes. Both processes are closely linked to local flow phenomena in the carotid artery bifurcation. The study of the flow field in the carotid bifurcation is of great clinical interest with respect to the genesis and diagnosis of atherosclerotic disease [Ku *et al* (1989)].
Previous studies of steady flow in the carotid artery bifurcation have shown that many flow phenomena, such as flow separation, reversal flow and curvature effects are important. Near the non-divider wall flow separation occurs, resulting in a region of reversed flow. Near the divider wall a region of high axial shear with high axial velocities is separated from the reversed flow region by a shear layer. A secondary flow that shows a helical structure (figure 2) can be found in the region of reversal flow.

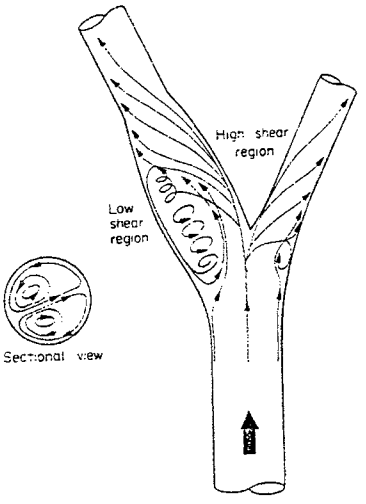

Figure 2, Schematic representation of the flowfield of the human carotid bifurcation (Bharadvaj)

These helical flow trajectories show a great resemblance with Dean vortices found in bends [Rindt (1989)]. The high velocities at the divider wall and the low velocities at the non-divider wall are seperated by a high velocity gradient in the shear layer. Therefor it is clear that the flow in the human carotid artery bifurcation is highly complex.
Studies of the unsteady, pulsatile Newtonian flow [Palmen (1994)] showed that, although many phenomena are comparable with the steady state results, there are a few important differences. In the acceleration phase of the flow the flow reversal region fully disappears. The velocity profile is positive across the entire lumen. In the deceleration phase a region with flow reversal develops at the non-divider wall of the sinus in the internal branch. Due to the negative velocity in this region and the high axial velocity near the divider wall there is a significant shear layer with high velocity gradients in the boundary layer between the two regions. A small vortex is developed in the shear layer.
Blood is a concentrated suspension of bloodcells in plasma. Therefor it exhibits non-Newtonian properties such as shear thinning and visco-elasticity. The influence of the non-Newtonian properties of blood is studied by several groups. Perktold has shown in his study of non-Newtonian flow in the carotid artery bifurcation that shear thinning has small influence on the flow field. In bends the non-Newtonian properties of blood cause lower wall shear rates and less reversal flow at the inner side of the bend [Mann, Tarbell (1990)]. For that reason it is important to study the influence of non-Newtonian properties of blood on the flow in artery models. Research in the Atherosclerosis project at the Eindhoven University of Technology until now was concentrated on the study of Newtonian flow in carotid bifurcation models e.g. [Rindt (1989), Palmen *et al* (1992)]. LDA experiments in a 1:1 model of the carotid bifurcation have shown a non-negligible difference in the steady flow field caused by the viscoelastic properties of the blood-like fluid [Zuidervaart (1995)]. In this study a visualization study of pulsatile flow in a 5:1 enlarged model of the human carotid artery is performed with the hydrogen bubble visualization method. The purpose of the study is to determine the influence of the non-Newtonian properties of blood on the flow. For that reason, two

experiments have been done: the first with water as Newtonian fluid and the other with a Xanthangum solution as non-Newtonian fluid.

2. Materials and methods

2.1. Model of the bifurcation

The experiments have been performed in a 5:1 model of the carotid artery bifurcation machined out of perspex (PMMA) as shown in figure 1. The geometry of the rigid three-dimensional model of the carotid artery bifurcation is based upon the data of Bharadvaj *et al* (1982). It is the same model used in the study of Palmen (1994).

2.2. Visualization of the flow

The hydrogen bubble visualization method has been used to visualize the flow in the carotid artery bifurcation. This method is very suitable to provide qualitative information about the flow in space and time. It gives a global view of the velocity profiles in the flow. The principle of the hydrogen bubble visualisation method is that little bubbles of hydrogen are convected by the passing fluid, visualizing the velocity profiles of the flow. The bubbles are generated by the electrolysis of water. The chemical reaction of this process is described by:

cathode: $4H_2O + 4\,e^- \rightarrow 2H_2 + 4OH^-$

anode: $2H_2O - 4\,e^- \rightarrow O_2 + 4H^+$

There are some limitations to this method: (*i*) the frequency of the velocity fluctuations that can be visualized properly is limited because of the inertia of the hydrogen bubbles, (*ii*) the size of the bubbles determines the spatial resolution of the method, (*iii*) the bubbles are displaced from the fluid path line by the buoyancy forces. This buoyancy forces are proportional to the square of the diameter of the bubbles.
The hydrogen bubbles have to be as small as possible for the following reasons:

- to reduce the buoyancy forces
- to increase the spatial resolution
- to increase the maximum frequency of the velocity fluctuations that can be followed by the bubbles

In order to generate the hydrogen bubbles, very thin platina wires are placed in the bifurcation as cathode and a gilded anode is placed downstream the internal branch. Because the hydrogen

bubbles are much smaller than the oxygen bubbles, the cathode is placed in the measuring section and the anode is placed downstream in the internal branch.
The electrodes are placed in the plane of symmetry, because the velocity perpendicular to this plane is zero. From Palmen (1994) it follows that in order to get good results with this method, the cathode wire's diameter has to be very small (20 μm) and the voltage has to be low (30 V.). The voltage is supplied in form of square wave pulses with a frequency of 0.014 Hz. and a duration of 0.10 sec. In this way the bubbles will form discrete lines and show the velocity profiles of the flow. To generate the square wave pulses Labview is used. The generation of the bubbles is triggered with the flowpulse: at the beginning of each flowpulse a triggerpulse is send to Labview to start the generation of the bubbles.

2.3. Blood Analog fluid

Blood is a complex non-Newtonian fluid, having shear rate and time dependent viscous and elastic properties. Looking at the microscopic structure of blood the shear thinning and viscoelastic behavior is explainable. Blood is a concentrated suspension of red blood cells (RBC), white blood cells (WBC), platelets and other cells as cholesterol in a fluid called plasma. The RBC are the most imported reason for the non-Newtonian properties of blood, due to their high volume concentration (45%). Although the WBC are larger then the RBC, and the platelets are quite numerous, their volume concentration is much less then that of the RBC (1%). It can be said that blood behaves like a Newtonian fluid (plasma) with flexible asymmetrical particles (RBC) suspended in it. The deformation and orientation of the flexible RBC in flow direction at high shear rates causes shear thinning. At low shear rates shear thinning is caused by aggregation of the blood cells. Therefor also time constants related to viscoelasticity will characterize the flow behavior.
The fluid used in the experiments as non-Newtonian blood analog fluid has to resemble the rheological properties of blood. Furthermore it has to be transparent with reference to the visualization method used. In his report Zuidervaart has found a fluid that satisfies this demands. On the ground of his results the experiments are done with a solution of water with 250 ppm Xanthangum. Xanthangum is a natural polysaccharide, with a three-dimensional structure that looks like a double helix which aggregates to a stiff rod like macromolecule. The viscosity of the solution has been tested on a viscometer.
The results are plotted in the figures below with the results of blood [Thurston (1979) and Cokelet (1980).

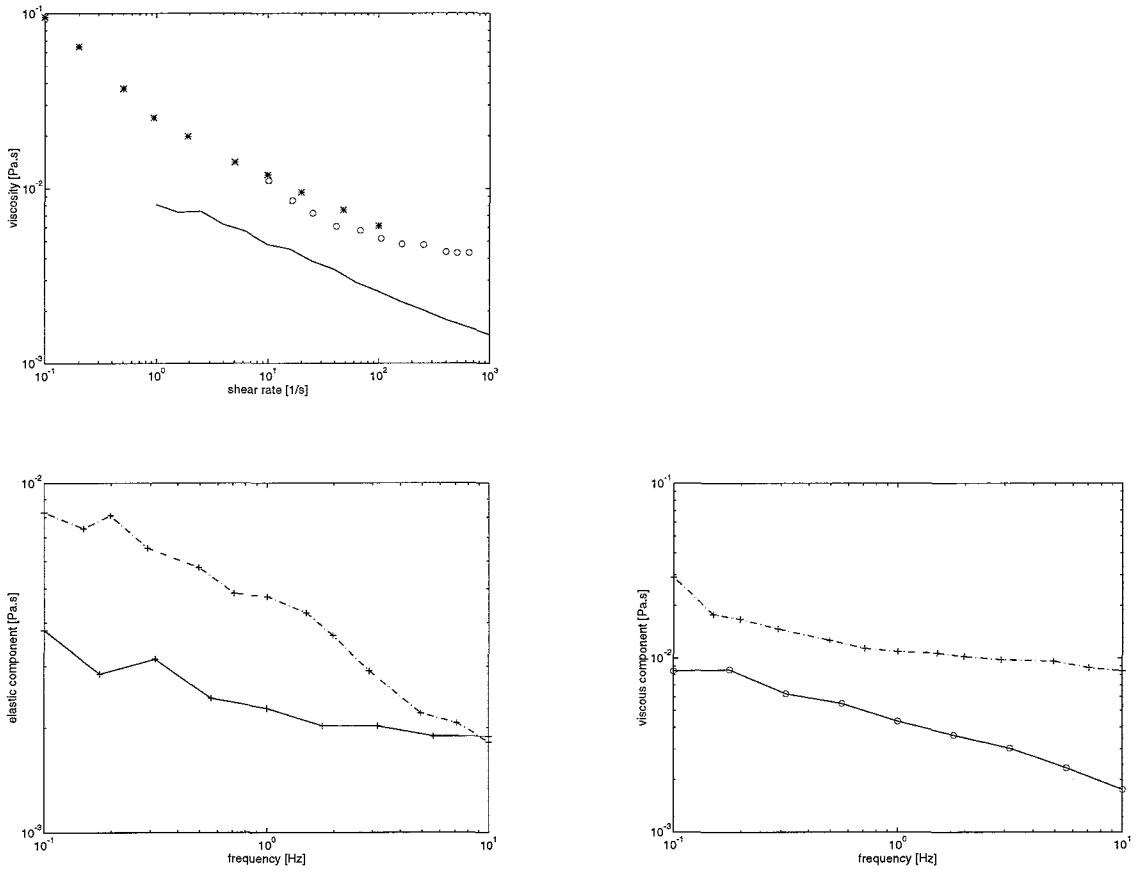

Figure 3, Elastic component of the complex viscosity-frequency of blood and Xanthangum (left), the viscous component-frequency of blood and Xanthangum (right) with '-' = Xanthangum, '-.' = blood and steady shear-viscosity of blood and Xanthangum (above) with '-' = Xanthangum,'' = blood (Merrit et al) , 'o' =blood (Cokelet))[Thurston (1979),Cokelet (1980)]*

As shown in the figure above the non-Newtonian fluid used is shearthinning and viscoelastic. The viscosty at low shear rates of Xanthangum is less than the viscosity of blood, although the trend is followed. The viscosity of Xanthangum at high shear rates ($\dot{\gamma} \rightarrow \infty$) goes to the viscosity of water. The elastic component of the viscosity is also less than that of blood, just like the viscous component of the viscosity, but the trend is still followed.
This means that the non-Newtonian properties of blood are overestimated in the fluid used, but the fluid can be used to give qualitative information about the non-Newtonian flow.

2.4. Experimental set up

A schematic representation of the experimental setup is given in figure 4.

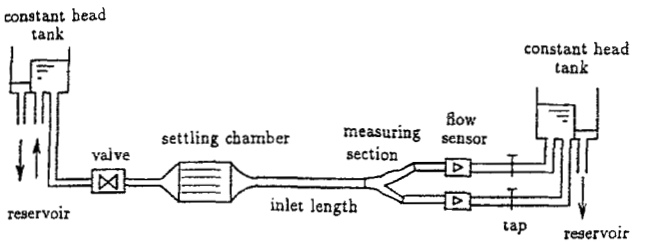

Figure 4, schematic representatation of the experimental setup

The flow system provides steady flow between two constant head tanks. An adjustable valve is controlled by a steppenmotor and a PC, to obtain the required flowpulse. From the upstream tank the fluid passes a settling chamber and a number of flowstraighteners to ensure a stable flow at he entrance of the inlet tube. To be sure that the steady and unsteady velocity profiles are fully developed at the measuring section, the length of the inlet tube is approximately 30D. D represents the diameter of the common carotid artery, being 40 mm. The flow is measured with electromagnetical flowmeters (Skalar instruments transflow 601) , placed after the valve and in the internal carotid artery. For that reason a little salt is added to the fluid. The flow ratio between the internal and the external branch can be adjusted by means of a tap in the external branch. After the fluid passes the downstream tank it is collected in a large reservoir from which the upstream tank is refilled again.
The platina cathode wires are placed in the measuring section as shown in figure 5.

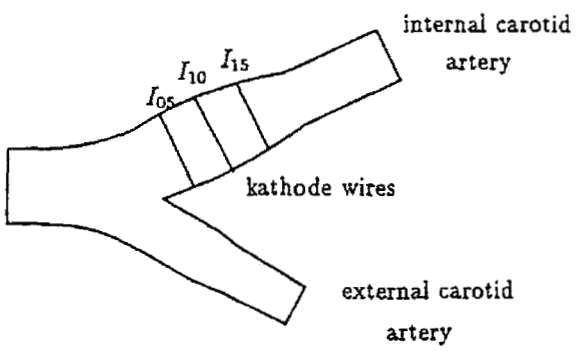

Figure 5,Position of the cathode wires in the measuring section

The hydrogen bubbles are made better visible by illuminating the measuring section from behind. The velocity profiles shown by the bubbles are recorded on a video tape.

2.5. Experimental procedures

The physiological flow conditions can be defined by three dimensionless numbers, being the Reynolds number (Re), the Womersley number (α) and the flow division ratio (γ). They are defined as follows:

$$\mathrm{Re} = \frac{DU_0}{\nu}, \quad \alpha = R\sqrt{\frac{\omega}{\nu}} \quad \text{and} \quad \gamma = \frac{Q_E}{Q_C}$$

With D representing the diameter of the common carotid artery (CCA), U the average velocity in the CCA, ν the kinematic viscosity (for the viscosity of the non-Newtonian fluid is taken the viscosity at $\dot{\gamma} \to \infty$, which is equal to the viscosity of the Newtonian fluid), R= D/2, $\omega = \frac{2\pi}{T}$ with T the period time of the flow pulse and Q_E, Q_C the flow through the external carotid artery and the common carotid artery.

For visco-elastic flows not only the Reynolds number, but also the Deborah number (De) and the Weissenburg number (We) are important. The linear viscoelastic behavior of the non-Newtonian fluid can be modelled with a Maxwell model as follows:

$$\lambda\dot{\boldsymbol{\sigma}} + \boldsymbol{\sigma} = 2\eta_0\mathbf{D}$$

To compare the flow of the non-Newtonian fluid in the carotid artery model with the flow of blood in a human carotid artery the dimensionless form of the Maxwell equation is used:

$$De\,\dot{\boldsymbol{\sigma}}^* + \boldsymbol{\sigma}^* = 2\mathbf{D}^*$$

with $\boldsymbol{\sigma}^*$, $\mathbf{D}^*$ resp. the dimensionless stress and deformation

To scale the non-Newtonian experiments correctly the Deborah numbers and the Weissenberg numbers of blood and the Xanthangum solution have to be equal. They are defined as

$$\mathrm{De} = \frac{\lambda}{\theta}, \quad \mathrm{We} = \lambda\frac{U}{D}$$

with λ the characteristic time of the fluid, θ the characteristic time of the flow, U the characteristic velocity of the flow and D the diameter of the artery. The characteristic time of the non-Newtonian fluid is [Bird *et al*]

$$\lambda = \left.\frac{\eta''/\omega}{\eta'}\right|_{\omega\to 0}$$

with η' and η'' following from the viscometer measurements (Figure 3).

	blood	Xanthangum
U	15 cm/s	2.5 cm/s
ω	6.3 rad/s	0.089 rad/s
D	1 cm	4 cm
λ	0.06	0.33 s

table 1, Characteristics of blood [Sharp] and xanthum gum

With the data in table 1 is found:

$$De_{blood} = 0.38 \text{ and } We_{blood} = 0.9$$
$$De_{xg} = 0.029 \text{ and } We_{xg} = 0.2$$

If the Deborah number is high, the elastic forcees dominate and if the Deborah number is small the viscous forces dominate. In this case the Deborah number of blood is larger than the Deborah number of Xanthangum, thus the elastic forces have at the flow of blood in the human carotid artery bifurcation more influence than at the non-Newtonian flow in the carotid bifurcation model used in the experiments. During the experiments the flow division ratio γ is kept constant ($\gamma = 0.45$). The Reynolds number varies during the flow period: Re = 300 during the diastole, Re = 1000 at the peak of the systole. The Womersley parameter is $\alpha = 6$. These parameters are in the experiments with water the same as in the experiments with the Xanthangum solution, to ensure the flow conditions are the same in the experiments. That way it is possible to determine the influence of the non-Newtonian properties.
The flowpulse used in the experiments is a simplification of the physiological flowpulse [Palmen (1994)]. The flowpulse is shown in figure 6.

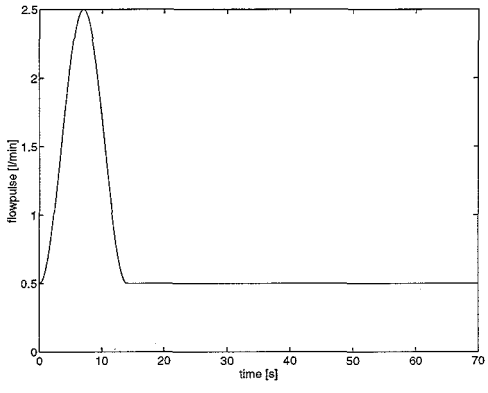

Figure 6, Flowpulse

The experiments are done with the Newtonian fluid and the non-Newtonian fluid. The flow is measured and the data is processed with *Labview*. The pulses for the hydrogen bubbles generation are also generated by *Labview*.
At each electrode wire the velocity profiles are recorded with a camera during one period. The velocity profiles of the Newtonian fluid are compared with the profiles of the non-Newtonian fluid.
For the non-Newtonian experiments the polarity of the electrodes had to be switched because the hydrogen bubbles were very large compared with the Newtonian experiments and sticked to the wires. After switching the polarity the bubbles showed the velocity profile very good. There is no explanation of this effect. Pictures of the videotape are made with TIM. Because the velocity profiles were not well visible at the pictures made with TIM, the velocity profiles are printed directly from the video screen.

3. Results

The velocity profiles are a function of time and will be described for the Newtonian and the non-Newtonian experiments. First the results of the Newtonian experiments will be described. The left hand side of figure 7 represent the visualization results for the Newtonian fluid. The pictures represent several phases of the flowpulse.
At the end of the diastolic phase (t/T = 0) the velocity profile is almost the same as in the steady flow situation. The velocities are positive over the entire profile.
At the peak of the systole (t/T = 0.10) the velocities are positive over the entire diameter. The velocity at the divider wall is higher than at the non-divider wall. The shear rates are high at the side of the divider wall and low at the non-divider side.
During the deceleration of the systole (t/T = 0.15) an area of low shear rates occurs at the non-divider side of the sinus. At t/T= 0.15 the high velocities at the divider side of the sinus become stronger and in the center of the sinus a shear layer occurs. At the non-divider wall the axial velocities are negative.
At the end of the systole (t/T= 0.20)in the low shear region the axial velocities become more negative. The shear layer becomes more pronounced and shifts to the divider side.
In the initial phase of the diastole (t/T = 0.23) the shear layer becomes instable and downstream a small vortex occurs. In the central part of the low shear region small positive velocities can be seen. Halfway the diastolic phase the shear layer becomes stable again and the vortex is downstream the sinus.

The right hand side pictures in figure 7 shows the non-Newtonian situation. At some points the flow shows significant differences with the Newtonian results.
The steady state of the non-Newtonian flow is more uniform distributed over the lumen.
At the peak of the systole the non-Newtonian flow profile shows little differences with the flow profile of the Newtonian fluid. Over the entire lumen the axial velocities are positive, at the divider wall the velocities are higher than the velocities near the non-divider wall.
During the deceleration phase of the systole the velocities in the low shear region are very small and the region of high velocities near the divider wall is small. During the deceleration the velocities are still positive although small over the entire lumen. The flow is more uniform over the lumen than during the Newtonian situation.
At the end of the systole the difference between the two fluids become more evident. A region of reversed flow occurs near the non-divider wall. In the center of the diameter the so called shear layer is less clear and there is no onset of a vortex. The shear layer shows a smaller shift towards the divider wall during the end of the systole and the initial phase of the diastole. At the region of reversed flow the flow is more uniform.
The transition to the steady flow situation in the diastolic phase occurs in the first half of the diastolic phase.
Although not shown in figure 7 the viscoelastic flow in the communis differs from the Newtonian flow. During the diastole the small regions of reversed flow near the walls are not present in the non-Newtonian flow.

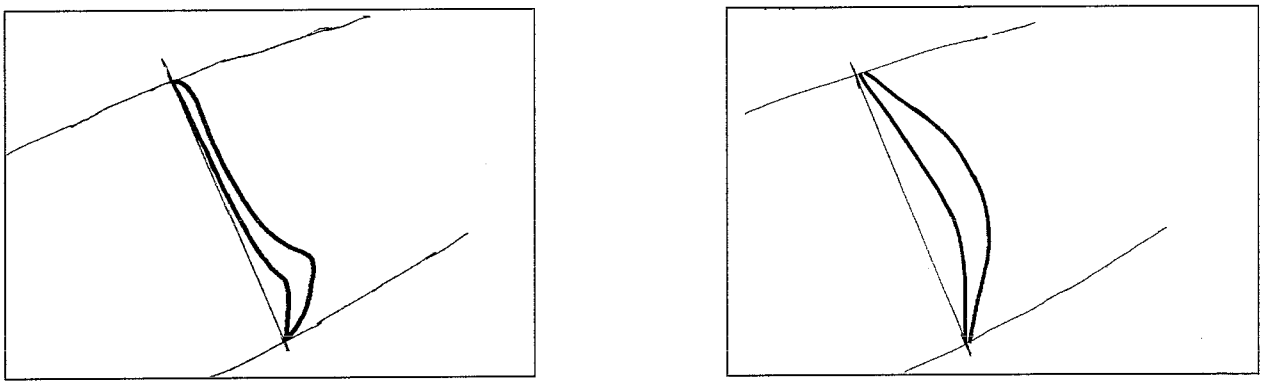

t/T= 0

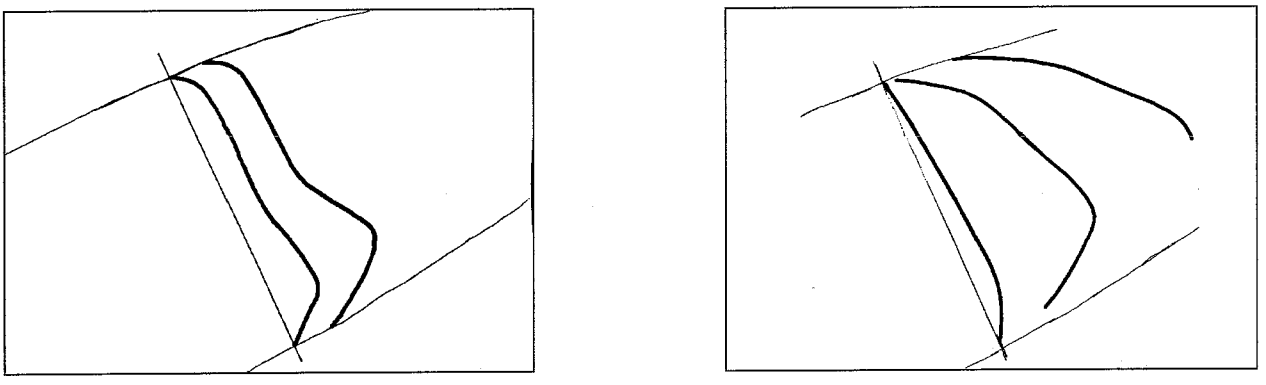

t/T = 0.10

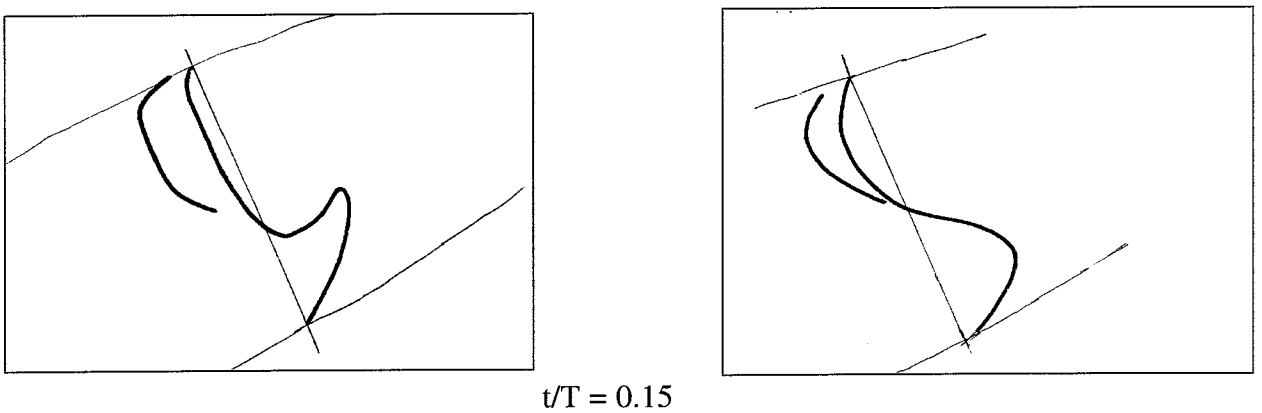

t/T = 0.15

Figure 7, Visualization results of the Newtonian fluid (left) and the non-Newtonian fluid (right) in the carotid bifurcation model

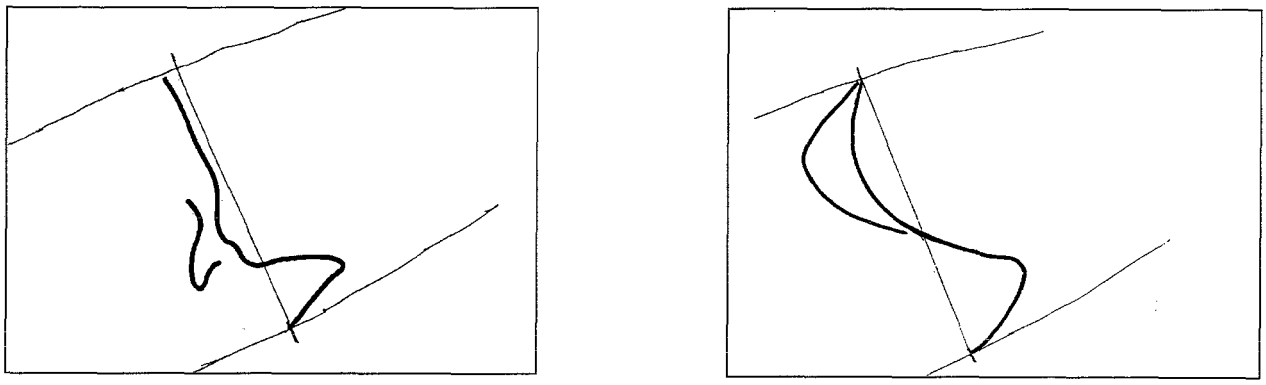

t/T = 0.2

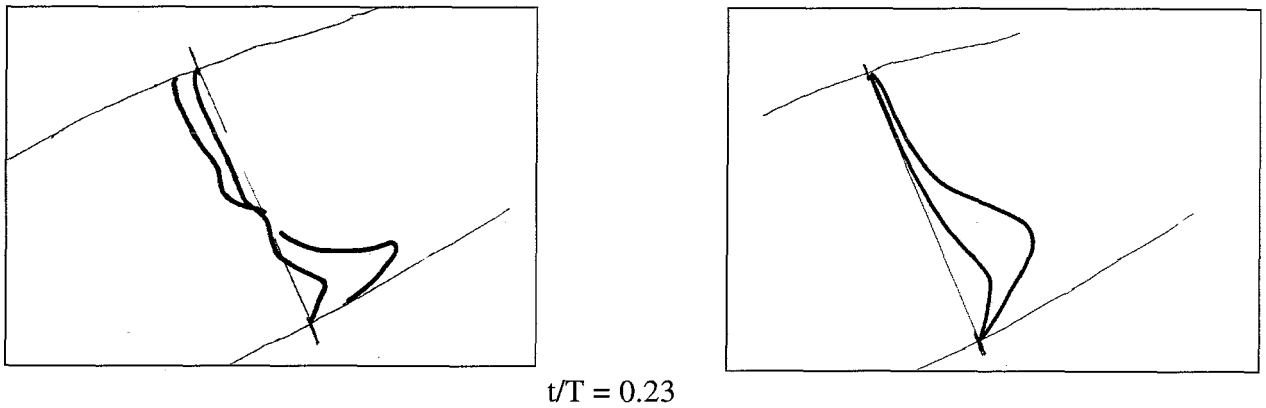

t/T = 0.23

Figure 7, continued

4. Discussion and conclusion

The dominant force on the hydrogen bubbles in the fluid is the drag force due to the local fluid motion. Due to the buoyancy forces the hydrogen bubbles have also a rise velocity. This velocity is dependent of the density of the particle, the density of the fluid and the dynamic viscosity of the fluid, expressed by Straub et al (1965) as

$$u_{rise} = \frac{(\rho_f - \rho_p)g}{18\nu} D_p^2$$

with ρ_p and ρ_f representing the density of the particle and the fluid respectively, D_p the diameter of the particle (estimated smaller than 100 μm), g the gravitational acceleration and ν the dynamic viscosity of the fluid ($\nu_{Newt} = 10^{-3}$ Pa.s, $\nu_{non\text{-}Newt} = 2 \cdot 10^{-3}$ Pa.s). Substituting these

values , it follows that $u_{rise} \approx 5$ mms^{-1} for the Newtonian fluid and $u_{rise} \approx 2.5$ mms^{-1} for the non-Newtonian fluid. This rise velocity causes an error in the axial velocities found in the experiments.The rise velocity of the bubbles in the non-Newtonian fluid is smaller than in the Newtonian fluid. The error in the axial velocity due to the rise velocity is less in the non-Newtonian fluid. The influence of the buoyancy forces is greater at low velocities as occur in the low shear region during the diastolic phase. This means that there is a difference between the motion of the hydrogen bubbles and the local fluid motion. Despite of this error the results of the visualizations still give qualitative information about the large scale flow phenomena. Since the flow conditions are the same for both experiments (the flow division ratio is constant) it is possible to compare the experiments and determine the influence of the viscoelastic non-Newtonian properties.

In the Newtonian visualizations vortex formations in the sinus occurs in the initial phase of the diastole. In the deceleration phase of the systole an area of reversed flow can be seen which develops further during the rest of the systole. This result shows resemblance's with the results of the visualization experiments of Ku *et al* (1983). Also other examples of vortex formation in the sinus are found in the literature (Palmen, 1994).

The non-Newtonian visualizations show no vortex formation in the deceleration phase. The velocityprofiles are more uniform distributed over the lumen and the shear rates at te non-divider wall are higher during the diastolic phase. This corresponds with the results of Zuidervaart (1995). This result is in contradiction with the literature (e.g. Perktold, 1991).

The hydrogen bubble method only visualizes the flow in the plane of symmetry. The secondary flow in the plane of symmetry opposes the influence of the buoyancy forces.

The visualization with the hydrogen bubbles will give qualitative information about the flow in the plane of symmetry, despite the fact that the flow in the carotid sinus has a helical structure (Bharadvaj ,1982).

It can be concluded that there is a significant difference between the flow of a Newtonian fluid and a non-Newtonian fluid through a bifurcation.

Since the elastic properties of the non-Newtonian fluid are overestimated, it is necessary to do more research on the influence of the non-Newtonian properties of blood on the flow through the bifurcation.

5. References

- Bharadvaj B.K., Mabon R.F., Giddens D.P. (1982). Steady flow in a model of the human carotid artery bifurcation, *J. Biomechanics*, vol.15, 349-378.
- Bird R.B., Armstrong R.C. and Hassager O. (1987). Dynamics of polymer liquids 1
- Cokelet G.R.(1980). Rheology and hemodynamics. *Ann. Rev Physiol* 42: 311-324.
- Ku D.N., Giddens D.P., Zarin C.K. and Glagov S. (1985). Pulsatile flow and atherosclerosis in the human carotid bifurcation, *Atherosclerosis* 5, 293-302.
- Liepsch D. And Moravec S. (1984). Pulsatile flow of non-Newtonian fluid in distensible models of human arteries, *Biorheology* 21, 571-586.
- Mann D.E. and Tarbell J.M. (1990). Flow of non-Newtonian blood analog fluids in rigid curved and straight artery models, *Biorheology* 27, 711-733.
- Palmen D.E.M., van de Vosse F.N, Janssen J.D. and van Dongen M.E.H. (1994). Analysis of the flow in stenosed carotid artery bifurcation models–Hydrogen-bubble visualization, *J. Biomechanics* Vol. 27, 581-590.
- Palmen D.E.M. (1994). The influence of minor stenoses on carotid artery flow, *Ph.D. Thesis Eindhoven University of Technology*
- Perktold K., Resch M., Florian H. (1991). Pulsatile non-Newtonian characteristics in a three-dimensional human carotid bifurcation model, *Journal of Biomechanical Engineering* Vol. 113, 464-475.
- Rindt C.C.M. (1989). Analysis of the three dimensional flow field in the carotid artery bifurcation, *Ph.D. Thesis Eindhoven University of Technology*
- Schraub F.A., Kline S.J., Henry J., Rundstadler P.W. jr., Littell A. (1965). Use of hydrogen bubbles for quantitative determination of time-dependent velocity fields in low-speed water flows, ASME *J. Basic Engineering* 87, 429-444.
- Sharp M.K. (1994). The effect of blood viscosity on pulsatile flow in straight tubes.
- Thurston G.B. (1979) Rheological parameters for the viscosity, viscoelasticity and thixotropy of blood.
- Zuidervaart J. (1995). Influence of viscoelastic fluid behavior on the steady flow field in a three dimensional model of the human carotid artery bifurcation.